Energy Conversion Circuit Laboratory

Solar Energy 262 (2023) 111749

Contents lists available at ScienceDirect

Solar Energy

journal homepage: www.elsevier.com/locate/solener

Superellipse model: An accurate and easy-to-fit empirical model for photovoltaic panels

Tofopefun Nifise Olayiwola, Sung-Jin Choi *

Department of Electrical, Electronic and Computer Engineering, University of Ulsan, Ulsan, 44610, South Korea

ARTICLE INFO

Keywords:
Photovoltaic
Solar cell model
I–V curve

ABSTRACT

The accurate representation of the photovoltaic (PV) characteristic curves especially at maximum power point (MPP) are essential for the real-time performance evaluation of PV panels. Over the years, equivalent circuit models which are based on the conversion behavior of PV panels have been the only approach employed in its modeling, simulation, and analysis. However, since the resulting I–V characteristic equation is inherently nonlinear and implicit, the full range enumeration of the PV characteristic curves is usually obtained in a complicated way. Thus, this paper proposes a novel empirical model for modeling and analysis of PV panels. Due to the unique similarities between the geometric shapes of a superellipse and the graphical characteristics of the I–V curve, an explicit mathematical correlation describing the behavior of PV panels can be established. By outlining a step-by-step procedure, the parameter extraction procedures are illustrated. As a result, the straightforward description of the full-range parameter fitting extraction of the I–V curve is greatly simplified. To validate the superiority of the proposed model over the conventional single-diode model, the model accuracy is evaluated according to the IEC EN 50530 standard. The simulation results revealed that irrespective of PV panel specification, cell material, and ambient conditions, the proposed empirical model maintains a low absolute current and power errors within the vicinity of MPP.

1. Introduction

Solar energy remains a clean, reliable and affordable alternative to fossil fuel energy for achieving carbon neutrality [1–4]. To fully harness this abundant energy, photovoltaic (PV) panels are used for the conversion of this abundant light energy into electrical energy in the form of DC currents for the end user. Since most PV panels are usually installed at locations which are far away from the operator [5,6], its real-time performance analysis at various ambient conditions are quite difficult [7].

To address this challenge, equivalent models have been proposed in literature for the effective modeling, simulation and study of the behavior of PV panels. By taking advantage of the conversion principle of a typical PV panel, equivalent circuit models have been used and successfully implemented in various software environments such as PSIM, MATLAB/Simulink etc [8]. This equivalent circuit model can be classified based on the number of diode component present in the electrical circuit [9].

While the triple-diode or double-diode models consists of three or two diode components respectively, most researchers and technicians rely heavily on the single-diode model, as it contains the fewest number of electrical parameters, and a simpler I–V characteristic equation [10]. However, the implicitness and nonlinearity of these equations makes the accurate and rapid reconstruction of the PV characteristic curves very tedious.

Over the years, substitute or approximate single-diode photovoltaic model (PVM) equations have been proposed in literature [8]. These approximate PVM equations are transformed into explicit form by either the decoupling or parametrization of its exponential term. Based on their mathematical formulas, such approximate PVM equations can either be analytical-based or iteration-based [11]. Since the iteration-based PVM equations are heavily dependent on its initial guess values and specified tolerance, the accuracy of the approximate PV characteristic curves within the vicinity of maximum power point (MPP) are usually low [12–14].

The most widely used mathematical formula for the decoupling of the exponential term under the analytical-based PVM equation is the Lambert-Ω function [15]. In simple terms, it establishes an explicit relationship between the basic I–V characteristic equation and the real-branch values of $\Omega(x)$. Nonetheless, the basic Lambert-Ω method also known as Haley's method does not express the $\Omega(x)$ as an elementary

* Corresponding author.
E-mail address: sjchoi@ulsan.ac.kr (S.-J. Choi).

https://doi.org/10.1016/j.solener.2023.05.026
Received 26 December 2022; Received in revised form 11 May 2023; Accepted 17 May 2023
Available online 23 June 2023

equation [16,17]. Hence, several improvements in the form of approximate expansion formulas have been proposed in literature to obtain the values for $\Omega(x)$ [18–26].

Other PVM equations in literature that can be categorized under this group are Taylor's series expansion [27], Padé approximant [28,29], Symbolic function [30], Chebyshev polynomials [31], Two-port network expansion [32], and two parameter model [33,34]. Irrespective of the PVM equations employed in approximating the PV characteristic curves, its complexity, required numbers of parameters or information are all still a major limitation hindering the full understanding of the behavior of PV panels. Thus, this paper proposes a novel empirical model based on the graphical characteristics of the I–V curve as specified in a typical manufacturer's datasheet.

Due to the unique similarities between the I–V curve at standard test condition (STC) and the geometric shapes of a superellipse, a new empirical model describing the behavior of PV panel can be obtained. By applying the key datasheet constraints into this model, an explicit simultaneous equation describing the I–V curve is derived. Hence, the roots of these multidimensional equation automatically become the optimum fitting parameters required for the accurate modeling of the PV characteristic curves.

The structure of this paper is as follows. In Section 2, the conventional single-diode model, its characteristic equation and key points under varying conditions are discussed. Next, in Section 3, the theoretical background of proposed empirical model and its specific considerations under both STC and varying conditions are established. Based on this established fact, a step-by-step procedure for obtaining the optimum fitting parameters for the proposed model are derived in Section 4. In Section 5, the parameter convergence and model accuracy of the superellipse model are evaluated. Finally, conclusions and future works drawn from these results are given in Section 6.

2. Conventional modeling of the PV characteristic curves

2.1. Single-diode model

Due to its simplicity, the single-diode model as shown in Fig. 1(a) is widely used for evaluating the performance of PV panels as it contains only a diode component and five fitting parameters. By applying circuit analysis to Fig. 1(a), the I–V characteristic equation can therefore be expressed as

$$i_{pv} = I_{ph} - I_s \cdot \left[e^{\left(\frac{v_{pv} + i_{pv} R_s}{A N V_t} \right)} - 1 \right] - \frac{v_{pv} + i_{pv} R_s}{R_{sh}} \tag{1}$$

where i_{pv} is the instantaneous PV output current (A), v_{pv} is the instantaneous PV output voltage (V), I_{ph} is the photovoltaic current (A), I_s the saturation current of the diode (A), V_t is the thermal voltage (V), A is the ideality factor, while R_s, R_{sh} and N are the series resistance (Ω), parallel resistance (Ω), and number of cells in a series string inside the panel respectively.

By performing further analysis, the photovoltaic current I_{ph} has been further defined mathematically in literature as [35,36]

$$I_{ph} = \frac{G}{G_n} \left(I_{scn} + \beta_I (T - T_n) \right) \tag{2}$$

which makes I_{ph} entirely dependent on the irradiance G and temperature T levels of each solar panel, the terms of (2) are defined such that I_{scn} is the short-circuit current at STC ($T_n = 298.15$ K, $G_n = 1000$ W/m^2) while β_I is the temperature coefficient of I_{sc}.

Furthermore, another key component of (1) is the saturation current I_s which has been expressed mathematically as [37,38]

$$I_s = \frac{I_{scn} + \beta_I (T - T_n)}{e^{\frac{V_{ocn} + \beta_V (T - T_n)}{A V_t}} - 1} \tag{3}$$

where V_{ocn} is the open-circuit voltage at STC and β_V is the temperature coefficient of V_{oc}. By obtaining the numerical solutions to (1), the regeneration of the I–V curve can be achieved as shown in Fig. 1(b) with four key-points; open-circuit voltage V_{oc}, short-circuit current I_{sc}, voltage at MPP V_{mp}, current at MPP I_{mp}.

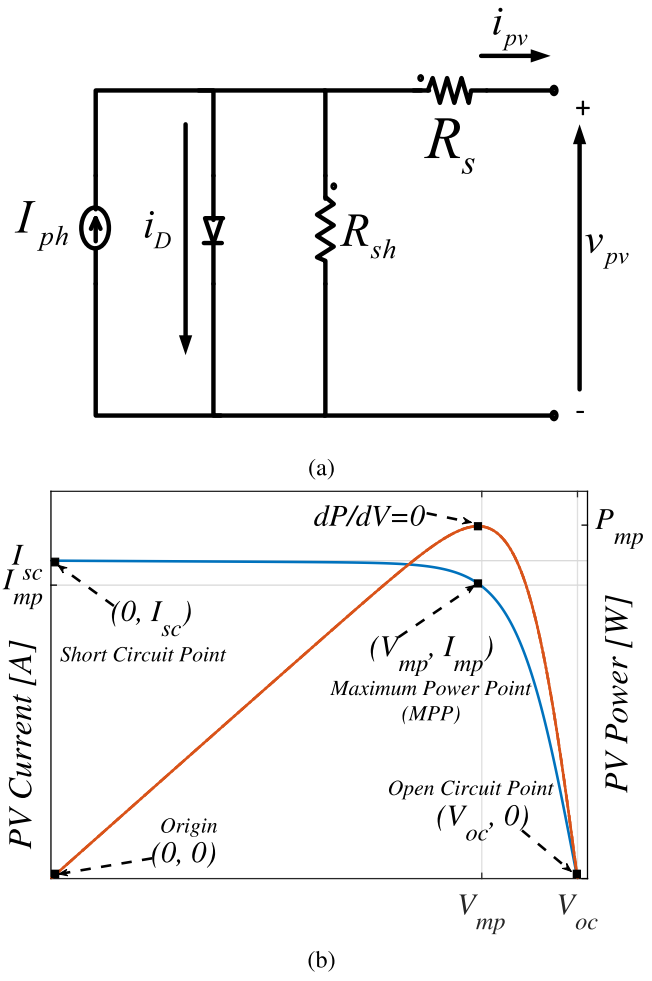

Fig. 1. Equivalent electrical circuit of the single-diode model and its corresponding characteristic curves under STC as obtained from a typical PV panel (a) single-diode model (b) key points of the I–V and P–V curves.

2.2. Effects of varying ambient conditions

However, (1) in its basic form does not describe the I–V curve under varying conditions. A change in the ambient conditions of a PV panel leads to corresponding changes to the key points of its I–V curve. The mathematical equation used in obtaining these estimated key points under this condition have been derived in literature as [39]

$$I_{sc} = I_{scn} \frac{G}{G_n} \left[1 + \beta_I (T - T_n) \right] \tag{4a}$$

$$V_{oc} = V_{ocn} + N A_n \frac{kT}{q} ln \left(\frac{G}{G_n} \right) + \beta_V (T - T_n) \tag{4b}$$

$$I_{mp} = I_{mpn} \frac{G}{G_n} \left[1 + \beta_{I,mp} (T - T_n) \right] \tag{4c}$$

$$V_{mp} = V_{mpn} + N A_n \frac{kT}{q} ln \left(\frac{G}{G_n} \right) + \beta_{V,mp} (T - T_n) \tag{4d}$$

where the quantities with subscript n denotes its value under STC. While A_n determines the squareness of the I–V curve, $\beta_{I,mp}$, and $\beta_{V,mp}$ has been approximated as [39]

$$\beta_{I,mp} \cong \beta_I, \beta_{V,mp} \cong \beta_V. \tag{5}$$

3. Superellipse modeling of the PV characteristic curves

3.1. Proposed model

A basic superellipse which is also known as a single-shaped superellipse is a geometric curve that always retains its x and y intercepts irrespective of distortion in its overall shape as shown in Fig. 2(a). Although, due to its single-shape constraint, the enumerated geometric curves are usually smoother, and well-rounded at both axes, it does not offer high flexibility in its overall shape.

On the other hand, in addition to retaining its intercepts, the geometric curves of a double-shaped superellipse at any given point as shown in Fig. 2(b) has more flexibility in its overall shapes. Thus, these geometric steep curves are usually more angular in shape with very steep slope when compared with the single-shaped superellipse. Hence, the implicit equation describing any point $P(x, y)$ along the curve can be expressed as

$$\left(\frac{x}{A}\right)^m + \left(\frac{y}{B}\right)^n = 1 \tag{6}$$

where A is the positive $x-$intercept value, B is the positive $y-$intercept value, m and n are its optimum fitting parameters.

If we take A and B as the V_{oc} and I_{sc} of a typical I–V curve respectively, a novel implicit equation for PV panels can be defined as

$$\left(\frac{v}{V_{oc}}\right)^m + \left(\frac{i}{I_{sc}}\right)^n = 1 \tag{7}$$

where i is the output current of the superellipse model and v is the output voltage of the superellipse model.

By making i the subject of the formula, an explicit equation describing the full-range enumeration of the I–V curve under STC can therefore be written as

$$i = I_{sc}\left[1 - \left(\frac{v}{V_{oc}}\right)^m\right]^{\frac{1}{n}}. \tag{8}$$

3.2. Consideration of varying ambient conditions

Similar to the typical I–V curve as described in Section 2.2, the key points of the superellipse model are also dependent on the ambient conditions of the PV panel. Thus, any variation in the irradiance or temperature leads to corresponding changes in the V_{oc} and I_{sc} points of (8).

Over the years, many researchers have successfully studied and proposed simplified mathematical equations for estimating the fixed axes points of the I–V curve under this condition [36]. Hence, the open circuit current I_{sc}^*, and short circuit voltage V_{oc}^* for the superellipse model under varying ambient conditions can therefore be estimated as

$$I_{sc}^* = I_{scn}\frac{G}{G_n} \tag{9a}$$

$$V_{oc}^* = V_{ocn} + NA_n\frac{kT}{q}ln\left(\frac{G}{G_n}\right) + \beta_V(T - T_n). \tag{9b}$$

Nonetheless, (9b) is still heavily dependent on the accurate estimation of A_n which usually ranges between $1 < A_n < 2$. Many researchers have proposed different techniques for obtaining this value with varying levels of complexity [40–42].

Based on the physics describing the behavior of PV panels, the typical I–V curve have been defined as a superposition of its diode characteristic curve [43]. Hence, A_n can therefore be considered as the reciprocal slope factor of the voltage ratio of the I–V curve, which in practice, characterizes the Shockley–Read–Hall recombination of the diode. Thus, a new simplified and quick mathematical equation for obtaining A_n in (9b) for any PV panel can therefore be expressed as

$$A_n = \frac{V_{oc}}{V_{mp}}. \tag{10}$$

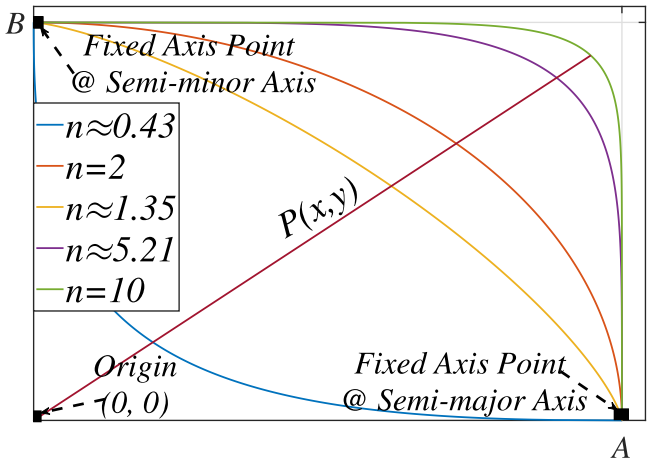

(a)

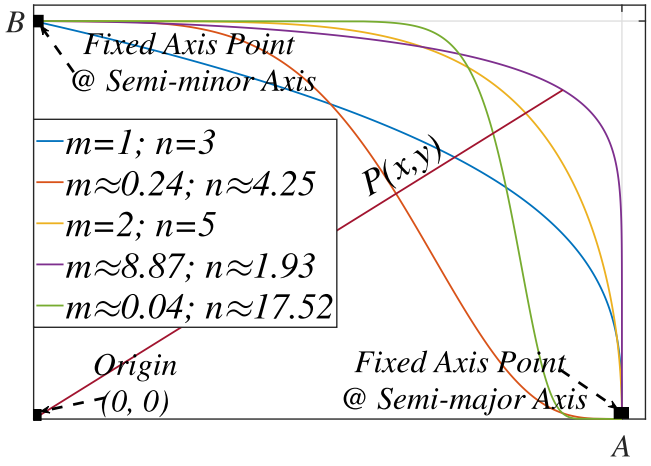

(b)

Fig. 2. Superellipse with varying parameter values (a) single-shaped superellipse (b) double-shaped superellipse.

Thus, by combining (9) into (8), the updated mathematical expression for obtaining the full range of the I–V curve under varying ambient conditions is expressed as

$$i = I_{sc}^*\left[1 - \left(\frac{v}{V_{oc}^*}\right)^m\right]^{\frac{1}{n}}. \tag{11}$$

4. Parameter extraction of the superellipse PV model

4.1. Finding the optimum fitting parameters

Due to the unique similarities between the conventional single-diode and the proposed models, we assume that the new model subsequently inherits all the mathematical properties and constraints describing the I–V curve. Thus, to ensure accuracy especially within the vicinity of MPP, and obtain its optimum parameters, the datasheet constraints are applied to the basic explicit equation describing the superellipse model (8).

(A) Constraint 1: The I–V curve starts from $(V_{oc}, 0)$ and ends at $(0, I_{sc})$. Hence, the fixed point of the superellipse model at both semi-major and semi-minor axes are the V_{oc} and I_{sc} points respectively.

(B) Constraint 2: The I–V curve must always pass through its MPP. Hence, by substituting the MPP values as obtained in any manufacturer's datasheet under STC into (8), an explicit equation describing MPP in the superellipse model can therefore be expressed as

$$I_{mp} = I_{sc}\left[1 - \left(\frac{V_{mp}}{V_{oc}}\right)^{m}\right]^{\frac{1}{n}}. \tag{12}$$

(C) Constraints 3: The slope of the P–V curve is null at MPP. Thus, the instantaneous power p of the superellipse model can therefore be defined as

$$p = i \cdot v. \tag{13}$$

To meet this constraint, we differentiate (8) such that

$$\left.\frac{dp}{dv}\right|_{v=V_{mp}} = i \cdot \left(\frac{dv}{dv}\right) + v \cdot \left(\frac{di}{dv}\right)\Big|_{i=I_{mp}, v=V_{mp}} = 0, \tag{14}$$

we obtain

$$I_{mp} = \frac{mI_{sc}}{n}\left(\frac{V_{mp}}{V_{oc}}\right)^{m}\left(\frac{I_{mp}}{I_{sc}}\right)^{1-n}. \tag{15}$$

By combining the Constraints 2 and 3, a simultaneous equation describing the novel nonlinear superellipse model can therefore be expressed as

$$I_{mp} = I_{sc}\left[1 - \left(\frac{V_{mp}}{V_{oc}}\right)^{m}\right]^{\frac{1}{n}} \tag{16a}$$

$$I_{mp} = \frac{mI_{sc}}{n}\left(\frac{V_{mp}}{V_{oc}}\right)^{m}\left(\frac{I_{mp}}{I_{sc}}\right)^{1-n}. \tag{16b}$$

Thus, (16) subsequently creates the exact conditions that must always be met to obtain the optimum fitting parameters of the empirical model.

4.2. Multi-variable Newton–Raphson Root-finding algorithm

Over the years, several parameter extraction algorithms have been proposed and successfully implemented in literature for obtaining the solutions to PV model multidimensional equations [44–47]. Methods such as Powell, Levenberg–Marquardt, and Newton–Raphson methods have all been effectively utilized in extracting the electrical parameters of the conventional single-diode model. The fast convergence and relative ease of the multi-variable Newton–Raphson method make it the suitable root-finding algorithm utilized in this paper [48,49].

To extract the fitting parameters, we rewrite (16) as composite functions

$$\begin{cases} f_1(m,n) = I_{mp} - I_{sc}\left[1 - \left(\frac{V_{mp}}{V_{oc}}\right)^{m}\right]^{\frac{1}{n}} = 0 & \text{(a)} \\ f_2(m,n) = I_{mp} - \frac{mI_{sc}}{n}\left(\frac{V_{mp}}{V_{oc}}\right)^{m}\left(\frac{I_{mp}}{I_{sc}}\right)^{1-n} = 0 & \text{(b)} \end{cases} \tag{17}$$

where f_1 and f_2 are functions with two independent variables. Next, we apply the first-order Taylor's series expansion about an initial point (m_0, n_0) such that

$$\begin{aligned} f_1(m_k, n_k) \cong f_1(m_{k-1}, n_{k-1}) &+ (m_k - m_{k-1})\left.\frac{\partial f_1}{\partial m}\right|_{(m_{k-1}, n_{k-1})} \\ &+ (n_k - n_{k-1})\left.\frac{\partial f_1}{\partial n}\right|_{(m_{k-1}, n_{k-1})} = 0 \end{aligned} \tag{18}$$

$$\begin{aligned} f_2(m_k, n_k) \cong f_2(m_{k-1}, n_{k-1}) &+ (m_k - m_{k-1})\left.\frac{\partial f_2}{\partial m}\right|_{(m_{k-1}, n_{k-1})} \\ &+ (n_k - n_{k-1})\left.\frac{\partial f_2}{\partial n}\right|_{(m_{k-1}, n_{k-1})} = 0. \end{aligned} \tag{19}$$

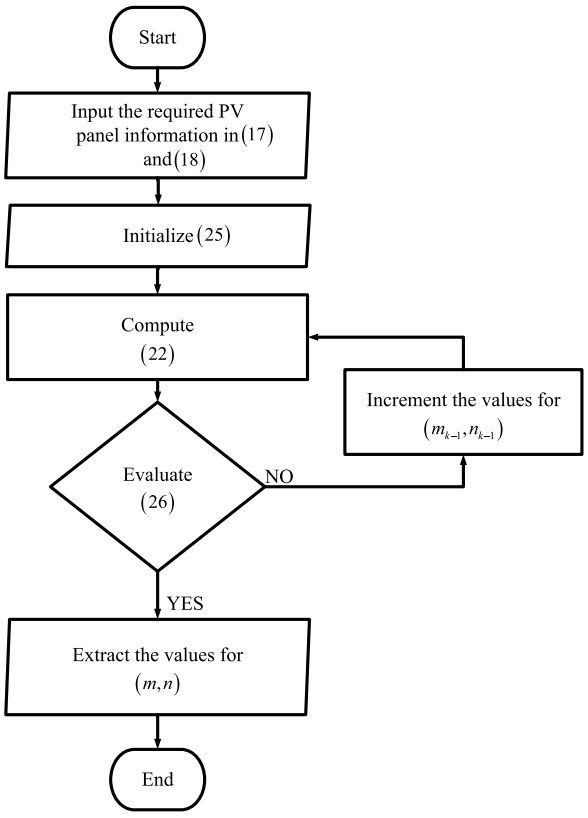

Fig. 3. A flowchart for the parameter extraction of the superellipse model for PV panels.

By re-arranging this equation into its matrix form, the values for m_k and n_k that meets

$$f_1(m_k, n_k) = f_2(m_k, n_k) = 0 \tag{20}$$

can therefore be extracted mathematically using

$$\begin{bmatrix} m_k \\ n_k \end{bmatrix} = \begin{bmatrix} m_{k-1} \\ n_{k-1} \end{bmatrix} - \begin{bmatrix} \frac{\partial f_1}{\partial m} & \frac{\partial f_1}{\partial n} \\ \frac{\partial f_2}{\partial m} & \frac{\partial f_2}{\partial n} \end{bmatrix}^{-1}_{(m_{k-1}, n_{k-1})} \begin{bmatrix} f_1(m_{k-1}, n_{k-1}) \\ f_2(m_{k-1}, n_{k-1}) \end{bmatrix} \tag{21}$$

where $k = 1, 2, 3, \ldots$ is the number of iterations, while Fig. 3 gives a detailed summary of the parameter extraction algorithm.

5. Parameter convergence and model accuracy

5.1. Criteria for evaluating accuracy

To evaluate the performance of PV characteristic curve approximations, the proposed empirical model is evaluated in accordance to the IEC EN 50530 standard. This standard maintains the notion that the absolute current and power errors within the vicinity of ±10% of the PV panel's V_{mp}, should always be less than or equal to 1%. The mathematical expression used in computing these absolute errors can therefore be expressed as

$$\varepsilon_I(\%) = \frac{1}{0.2V_{mp}}\int_{V_{mp}\pm 10\%}\left|\frac{i_s(v) - i_r(v)}{i_r(v)}\right| dv \times 100 \tag{22a}$$

$$\varepsilon_P(\%) = \frac{1}{0.2V_{mp}}\int_{V_{mp}\pm 10\%}\left|\frac{p_s(v) - p_r(v)}{p_r(v)}\right| dv \times 100 \tag{22b}$$

Table 1
PV panel specifications used in this paper.

Cell material	PV panel	V_{mp} (V)	I_{mp} (A)	V_{oc} (V)	I_{sc} (A)	β_I (A/°C)	β_V (mV/°C)
Multicrystalline	KC200GT	26.30	7.61	32.90	8.21	3.18×10^{-3}	-1.23×10^{-1}
Multicrystalline	CS6P-230P	29.60	7.78	36.80	8.34	65.00×10^{-3}	-3.40×10^{-1}
Monocrystalline	CS6X-305M	36.60	8.33	45.20	8.84	60.00×10^{-3}	-3.50×10^{-1}
CIGS Thin-film	Q.SMART UF L100	69.40	1.44	91.80	1.63	50.00×10^{-3}	-4.20×10^{-1}
Hybrid Thin-film	U-EA110	54.00	2.04	71.00	2.50	56.00×10^{-3}	-3.90×10^{-1}
Ultra-thin amorphous	VBHN330SA16	58.00	5.70	69.70	6.07	3.34×10^{-3}	-1.60×10^{-1}

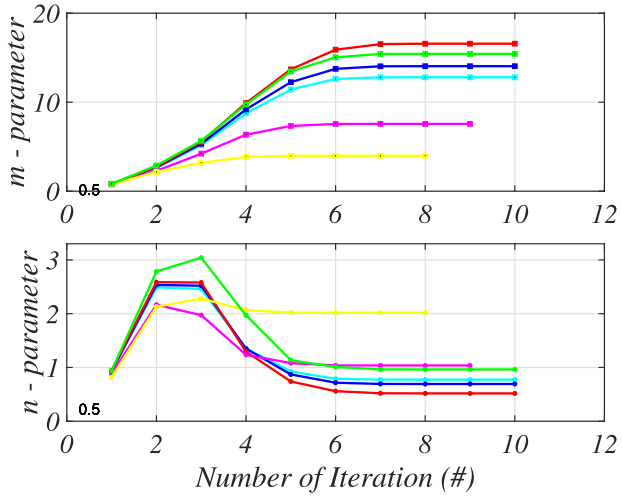

Fig. 4. A plot of the parameter convergence of the superellipse model for 6 different PV panels.

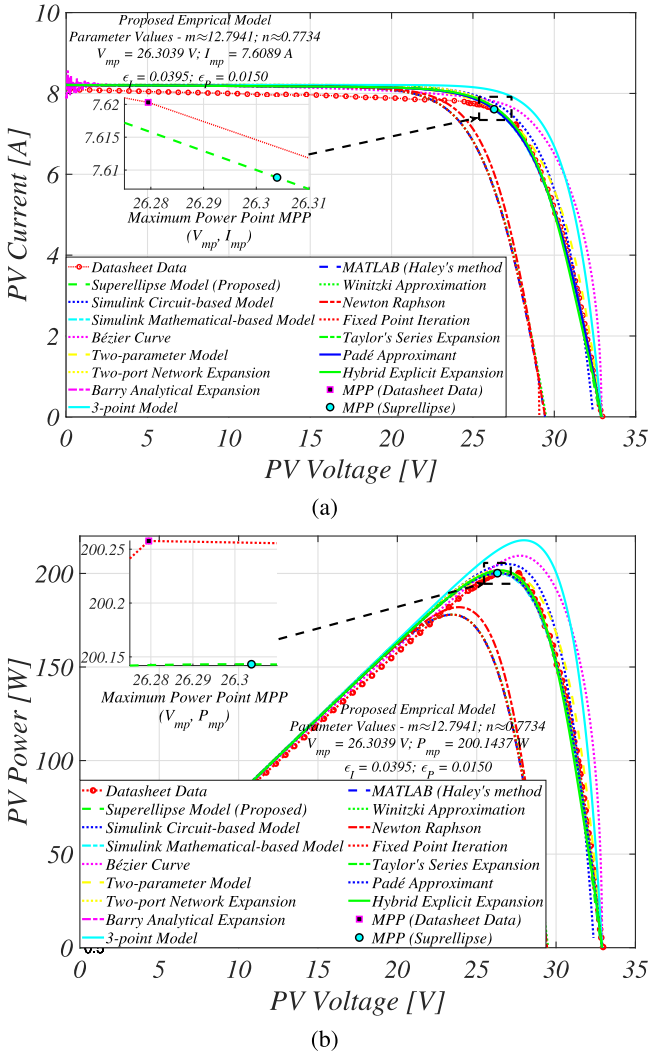

Fig. 5. Comparison of the proposed and the conventional single-diode PV models using the KC200GT PV panel (a) I–V curve (b) P–V curve.

where the subscript s represents the measured values of the approximate curves, and r denotes the data values from the reference model.

Since the performance evaluation is carried out using MATLAB/Simulink in an 11th Gen Intel(R) Core(TM) i9-11900K CPU, the PV characteristic curves obtained using the inbuilt Simulink circuit-based model [50] and its mathematical-based model [51] are also included in this analysis. Using the manufacturer's datasheet data as reference, the PV characteristic curves are therefore easily evaluated. According to literature, the KC200GT PV panel is the most widely used PV panel specification for the evaluation of various PVM equations. Thus, the newly proposed equation is compared with 14 conventional PVM equations at STC using KC200GT PV panel in Section 5.3.1. Then, in Section 5.3.2 the proposed empirical model are used to reconstruct the PV characteristic curves for 5 other PV panels with different materials as specified in Table 1. Finally, the performance of the empirical model under varying ambient conditions is examined in Section 5.4 using the KC200GT PV panel.

5.2. Parameter convergence

Since the simultaneous equation describing the superellipse model in (16) is inherently nonlinear, parameter convergence and numerical stability issues would arise if the initialization values for the multivariable Newton–Raphson's method are not well-defined. In practice, the fitting parameters of the standard ellipse is defined as

$$m = n = 2. \tag{23}$$

However, as established in Section 3.1, the fitting parameters of the superellipse model are dependent on the graphical characteristic of the I–V curve. Hence, by taking into account, the relationship establishing the voltage and current ratios of the typical I–V curve at STC, a mathematical expression for determining the initialization values (m_0, n_0) can therefore be expressed as

$$m_0 = \frac{V_{mp}}{V_{oc}} \tag{24a}$$

$$n_0 = \frac{I_{mp}}{I_{sc}}. \tag{24b}$$

In addition, to prevent non-convergence and infinite iteration, a termination condition is introduced into the algorithm as defined in

Table 2
Summary of the optimum superellipse fitting parameters for 6 different PV panels.

Cell material	PV Panel	Color	Model parameters		Iteration
			m	n	
Multicrystalline	KC200GT		12.7941	0.7734	10
Multicrystalline	CS6P-230P		14.0435	0.6926	10
Monocrystalline	CS6X-305M		16.6510	0.5174	10
CIGS Thin-film	Q.SMART UF L100		7.5611	1.0372	9
Hybrid Thin-film	U-EA110		3.8084	2.0840	8
Ultra-thin amorphous	VBHN330SA16		15.4235	0.9630	10

Table 3
Comparison of 15 different PVM equations for KC200GT PV panel within the vicinity of MPP.

Method	Reference	V_{mp} (V)	I_{mp} (A)	P_{mp} (W)	ε_I (%)	ε_P (%)
Datasheet Data		26.2795	7.6203	200.2577		
Superellipse Model (Proposed)		26.3039	7.6089	200.1437	0.0395	0.0150
Simulink Circuit-based Model	[50]	26.9240	7.6190	205.1341	0.0045	0.6404
Simulink Mathematical-based Model	[51]	26.4000	7.5802	200.1165	0.1392	0.0185
Padé Approximant	[28,29]	26.3463	7.5999	200.2306	0.0705	0.0036
Newton Raphson	[12]	23.8764	7.6217	181.9785	0.0048	2.4006
MATLAB (Haley's)	[16,17]	23.4482	7.5903	177.9804	0.1034	2.9257
Hybrid Explicit Expansion	[26]	26.4781	7.6162	201.6613	0.0143	0.1831
Fixed Point Iteration	[13]	23.4482	7.5904	177.9807	0.1033	2.9257
Barry Analytical Expansion	[25]	26.3463	7.5991	200.2083	0.0732	0.0065
Winitzki Approximation	[18,52]	23.4482	7.5908	177.9917	0.1021	2.9292
3 Point Model	[53]	27.9601	7.7874	217.7352	0.5766	2.2953
Two-Port Network Expansion	[32]	26.3860	7.6512	201.8837	0.1065	0.2136
Two-Parameter Model	[33,34]	26.7086	7.5045	200.4354	0.3996	0.0233
Taylor's Series Expansion	[27]	26.3793	7.5977	200.4230	0.0781	0.0217
Bézier curve	[11]	27.4431	7.6466	209.8464	0.0908	1.2593

(21) such that

$$m_k - m_{k-1} \leq \varepsilon_1 \tag{25a}$$

$$n_k - n_{k-1} \leq \varepsilon_2 \tag{25b}$$

with $\varepsilon_1 = \varepsilon_2 = 1 \times 10^{-6}$. These termination conditions ensure the solution of the simultaneous equation as defined in (17).

By directly substituting the required information from the PV panels specification in Table 1 into the root-finding algorithm as described in Fig. 3, the optimum fitting parameters are easily extracted. By utilizing (24) and (25), numerical stability and fast parameter convergence are always ensured as shown in Fig. 4 and as summarized in Table 2.

5.3. Accuracy evaluation under STC

5.3.1. Comparison with other PVM equations

By substituting the fitting parameter values of the KC200GT PV panel into (8), the data points required for the full range approximation of the I–V curve can therefore be easily obtained. Fig. 5 shows a comprehensive comparison of the newly proposed superellipse equation and 14 conventional PVM equations. While it is important to note that most of the recent PVM techniques in literature have high accuracy within the vicinity of MPP, extremely high absolute errors are observed in the older techniques - Newton–Raphson [12], MATLAB [16,17], Winitzki approximation [18,52], 3 point model [53].

The superellipse model as shown in Fig. 6 has the lowest absolute errors at both the current and power regions. Following closely are the Barry analytical expansion [25], Taylor's series expansion [27], Padé approximant [28,29] and the Simulink-based techniques [50,51]. This further validates the superellipse model as a powerful empirical model for understanding the nonlinear behavior of both the PV panel and its corresponding characteristics curves (see Table 3).

5.3.2. Application in different PV panels

Similarly, based on the explicit equation describing the superellipse model (8), the approximation of the PV characteristics curves for five other PV panels are examined. By substituting their fitting parameters in Table 2, into (8), the required data point values needed for the full-range enumeration and the corresponding key point values are as shown in Table 4.

The accuracy of the approximate PV curves as shown in Fig. 7 are then evaluated using the IEC EN 50530 standards with the manufacturer's datasheet data as a reference. It can be observed that irrespective of PV panel cell material and specifications, the superellipse model are very accurate thereby maintaining the 1% absolute error threshold within the vicinity of MPP as shown in Fig. 7(f).

5.4. Accuracy evaluation under varying ambient conditions

5.4.1. Constant STC temperature - varying irradiance conditions

Irrespective of the changes in ambient conditions, the optimum fitting parameters of the superellipse model remains unchanged. As such, the optimum values for m and n under STC are regarded as invariant. By applying (11), the full-range reconstruction of the KC200GT PV panel characteristic curves under constant STC temperature can therefore be achieved. As expected, the reconstructed I–V and P–V curves shown in Fig. 8 maintains high model accuracy at MPP with the datasheet curves as summarized in Table 5.

5.4.2. Constant STC Irradiance - varying temperature conditions

Similarly, the accuracy of the superellipse model is evaluated under varying temperature. Although the proposed model retains high accuracy up to 50 °C, high ε_P is observed in the reconstructed PV characteristic curves at 75 °C as shown in Fig. 9. Due to the constant STC irradiation, the estimated value for I_{sc}^{*} remains unchanged. Consequently, based on its mathematical equation, the value of I_{mp} will also remain the same as shown Table 5.

Table 4
Accuracy of the proposed method for 6 different PV panels.

PV Panel	Datasheet data			Model parameters		Superellipse approximation			IEC EN50530 standards	
	V_{mp}	I_{mp}	P_{mp}	m	n	V_{mp}	I_{mp}	P_{mp}	ε_I	ε_P
KC200GT	26.2795	7.6203	200.2577	12.7941	0.7734	26.3039	7.6089	200.1437	0.0395	0.0150
CS6P-230P	29.5194	7.7717	229.4159	14.0435	0.6926	29.6168	7.7756	230.2873	0.0134	0.1024
CS6X-305M	36.6685	8.3195	305.0623	16.6510	0.5174	36.6486	8.3273	305.1857	0.0268	0.0115
Q.SMART UF L100	70.1776	1.4073	98.7609	7.5611	1.0372	69.3784	1.4404	99.9358	0.8225	0.4154
U-EA110	54.7698	2.0200	110.0350	3.8084	2.0840	54.0140	2.0287	109.5765	0.1366	0.3046
VBHN330SA16	58.6183	5.6738	332.5882	15.4235	0.9630	57.9787	5.7021	330.6001	0.1628	0.1951

Table 5
Accuracy evaluation of the proposed model under varying ambient condition using KC200GT PV panel.

Ambient Condition (AC)		Datasheet Data (DD)			Superellipse Approximation (SM)			IEC EN 50530 Standards	
Irradiance (W/m^2)	*Temperature* (°C)	V_{mp}	I_{mp}	P_{mp}	V_{mp}	I_{mp}	P_{mp}	ε_I	ε_P
400	25	25.7354	3.0414	78.2716	25.0620	2.9910	74.9810	0.0802	0.9263
600	25	26.4015	4.5592	120.3697	25.3913	4.5666	115.9526	0.0429	0.9659
800	25	26.6890	6.1239	163.4408	25.9182	6.0848	157.7084	0.1682	0.9251
1000	25	26.2795	7.6203	200.2577	26.3134	7.6062	200.1463	0.0485	0.0146
1000	25	26.2795	7.6203	200.2577	26.3134	7.6061	200.1428	0.0490	0.0151
1000	50	23.7096	7.5154	178.1871	23.8540	7.6061	181.4365	0.3112	0.4701
1000	75	20.3147	7.5131	152.6264	21.3946	7.6061	162.7301	0.3108	1.6618

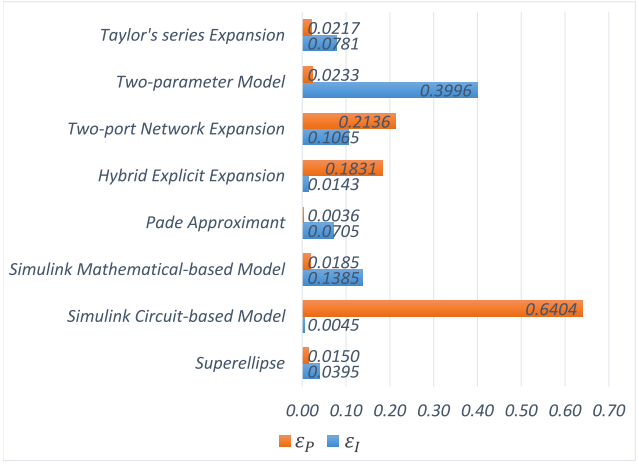

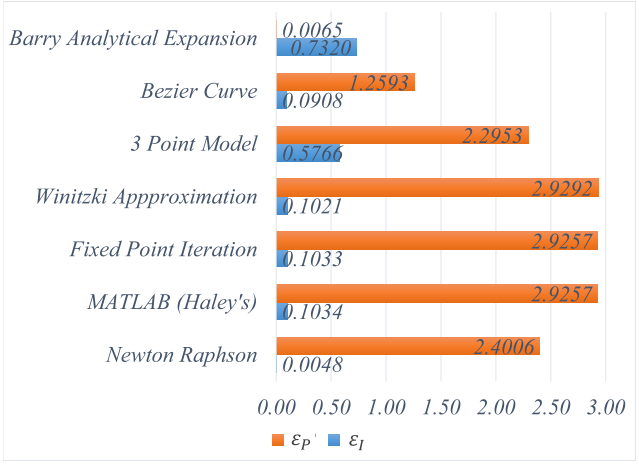

Fig. 6. Comparison of the model accuracy within the vicinity of MPP for 15 different PVM equations using KC200GT PV panel.

Regardless, this further adds to the numerous advantages of the superellipse model in achieving an easy-to-fit replica of both the I–V and P–V characteristic curves under both STC and varying ambient conditions.

6. Conclusion

In this paper, a novel empirical model is proposed for the performance evaluation of PV panels. Unlike the conventional single-diode model with 5 fitting parameters, the proposed model requires only three fitting parameters. By applying the well-established parameter extraction procedure, an explicit equation describing the full range approximation of the I–V curve is derived. This ensures that the roots of the simultaneous equation which are also the fitting parameters of the superellipse become easy to obtain. To evaluate the accuracy of this novel model, its reconstructed I–V and P–V characteristic curves were compared with 12 conventional PVM equations and 2 Simulink-based techniques describing the single-diode model according to the current and power errors near MPP.

From the simulation results and performance indices, it can be observed that irrespective of PV panel specification, ambient condition, and cell materials, accurate reconstruction of the PV characteristic curves especially at MPP is achieved. Due to the reduced number of model parameters, this model presents a simplified and novel insights into understanding the behavior, and performance of PV panels.

Declaration of competing interest

The authors declare that they have no known competing financial interests or personal relationships that could have appeared to influence the work reported in this paper.

Acknowledgments

This work was supported by the 2021 Research Fund of University of Ulsan, Korea.

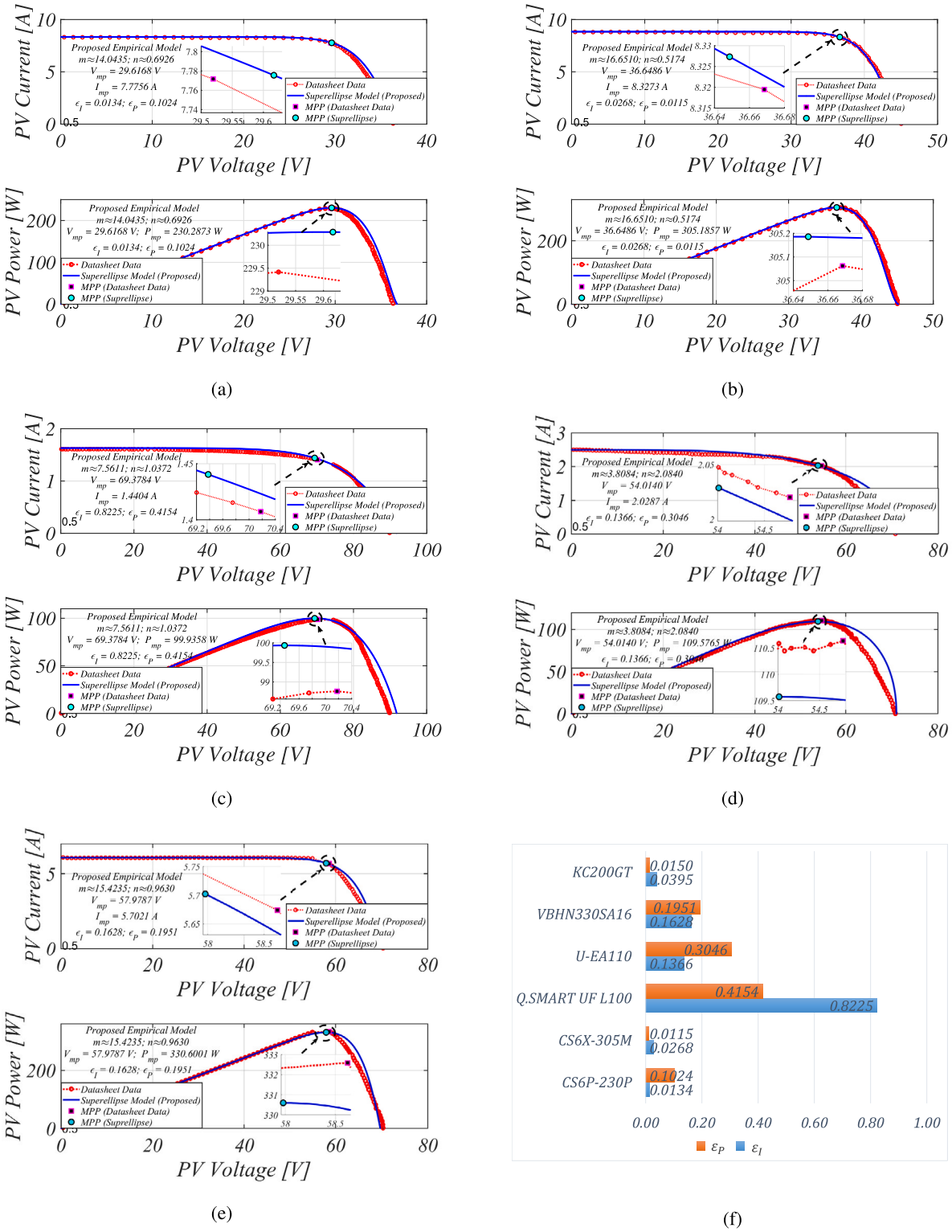

Fig. 7. Comparison of the PV characteristics curve approximation using the newly proposed superellipse model (a) CS6P-230P (b) CS6X-305M (c) Q.SMART UF L100 (d) U-EA110 (e) VBHN330SA16 (f) accuracy evaluation at MPP for 6 different PV panels.

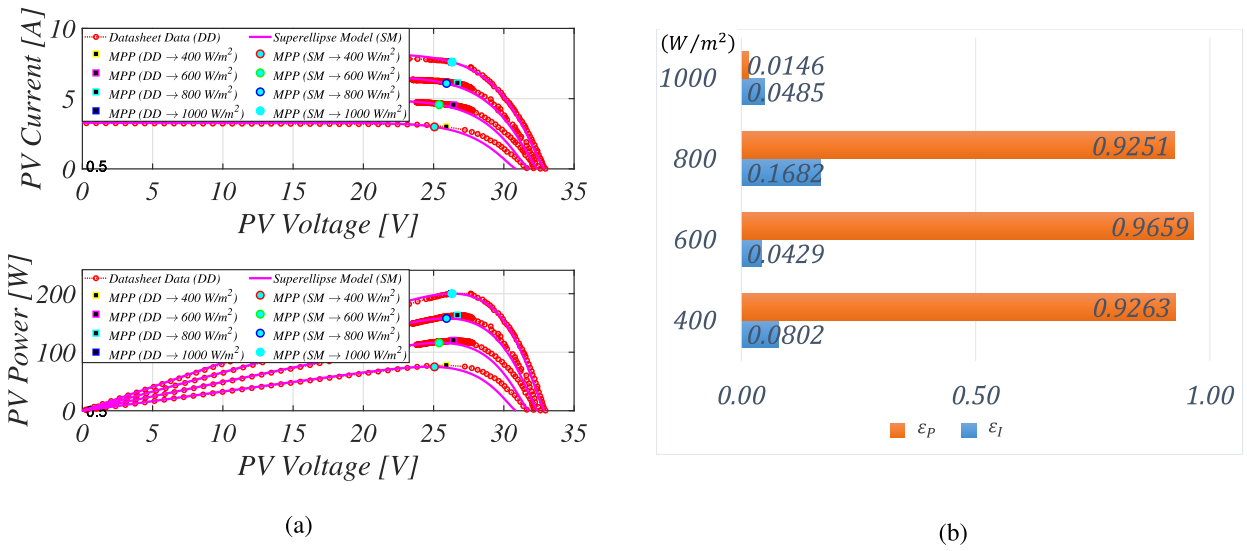

Fig. 8. Comparison of the performance of the superellipse model under constant STC temperature and varying irradiance conditions using KC200GT PV panel (a) PV characteristic curves (b) accuracy within the vicinity of MPP.

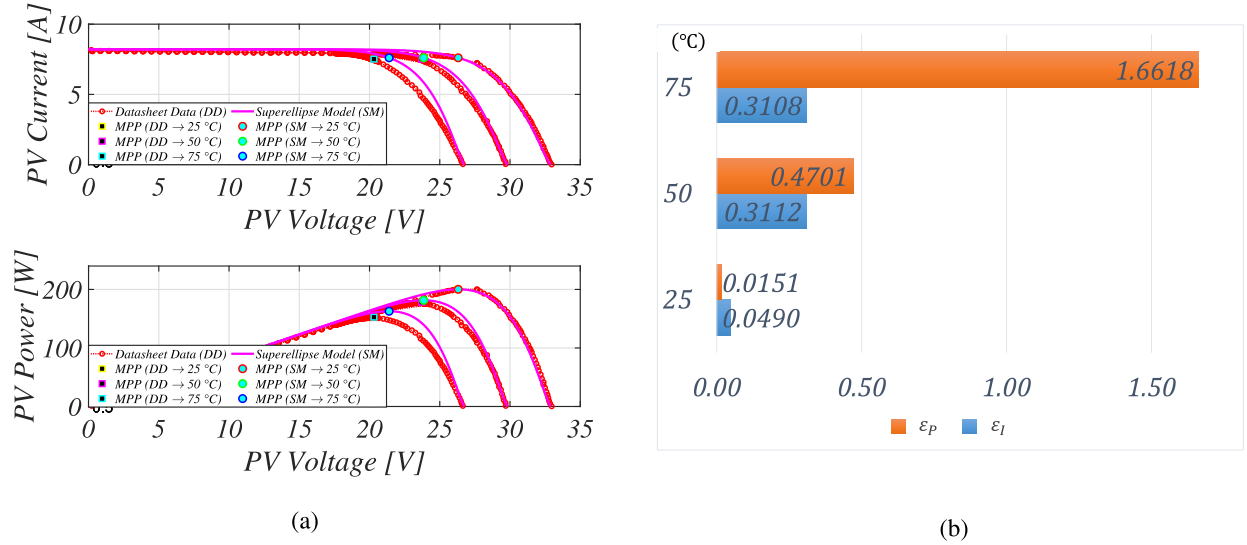

Fig. 9. Comparison of the performance of the superellipse model under constant STC irradiance and varying temperature conditions using KC200GT PV panel (a) PV characteristic curves (b) accuracy within the vicinity of MPP.

References

[1] F. Wang, J.D. Harindintwali, Z. Yuan, M. Wang, F. Wang, S. Li, Z. Yin, L. Huang, Y. Fu, L. Li, et al., Technologies and perspectives for achieving carbon neutrality, Innov. 2 (4) (2021) 100180.

[2] M. Vaka, R. Walvekar, A.K. Rasheed, M. Khalid, A review on Malaysia's solar energy pathway towards carbon-neutral Malaysia beyond COVID'19 pandemic, J. Clean. Prod. 273 (2020) 122834.

[3] N.Z. Muradov, T.N. Veziroğlu, "Green" path from fossil-based to hydrogen economy: an overview of carbon-neutral technologies, Int. J. Hydrogen Energy 33 (23) (2008) 6804–6839.

[4] G. Mutezo, J. Mulopo, A review of Africa's transition from fossil fuels to renewable energy using circular economy principles, Renew. Sustain. Energy Rev. 137 (2021) 110609.

[5] G. Makrides, B. Zinsser, M. Norton, G.E. Georghiou, M. Schubert, J.H. Werner, Potential of photovoltaic systems in countries with high solar irradiation, Renew. Sustain. Energy Rev. 14 (2) (2010) 754–762.

[6] M. Afolayan, T. Olayiwola, Q. Nurudeen, O. Ibrahim, I. Madugu, Performance evaluation of soiling mitigation technique for solar panels, Arid Zone J. Eng. Technol. Environ. 16 (4) (2020) 685–698.

[7] M.A. Hasan, S.K. Parida, An overview of solar photovoltaic panel modeling based on analytical and experimental viewpoint, Renew. Sustain. Energy Rev. 60 (2016) 75–83.

[8] S. Pranith, T. Bhatti, Modeling and parameter extraction methods of PV modules, in: 2015 International Conference on Recent Developments in Control, Automation and Power Engineering, RDCAPE, IEEE, 2015, pp. 72–76.

[9] A.M. Humada, M. Hojabri, S. Mekhilef, H.M. Hamada, Solar cell parameters extraction based on single and double-diode models: A review, Renew. Sustain. Energy Rev. 56 (2016) 494–509.

[10] S. Lineykin, M. Averbukh, A. Kuperman, An improved approach to extract the single-diode equivalent circuit parameters of a photovoltaic cell/panel, Renew. Sustain. Energy Rev. 30 (2014) 282–289.

[11] M. Louzazni, S. Al-Dahidi, Approximation of photovoltaic characteristics curves using Bézier Curve, Renew. Energy 174 (2021) 715–732.

[12] M. Uoya, H. Koizumi, A calculation method of photovoltaic array's operating point for MPPT evaluation based on one-dimensional Newton–Raphson method, IEEE Trans. Ind. Appl. 51 (1) (2014) 567–575.

[13] E.I.O. Rivera, F.Z. Peng, Algorithms to estimate the temperature and effective irradiance level over a photovoltaic module using the fixed point theorem, in: 2006 37th IEEE Power Electronics Specialists Conference, IEEE, 2006, pp. 1–4.

[14] R. Ayop, C.W. Tan, A.L. Bukar, Simple and fast computation photovoltaic emulator using shift controller, IET Renew. Power Gener. 14 (11) (2020) 2017–2026.

[15] E. Batzelis, Non-iterative methods for the extraction of the single-diode model parameters of photovoltaic modules: a review and comparative assessment, Energies 12 (3) (2019) 358.

[16] E.W. Weisstein, Lambert W-Function, Wolfram Research, Inc. 2002, https://mathworld.wolfram.com/.
[17] C. Moler, Cleve's corner: Cleve moler on mathematics and computing, 2012, Splines and Pchips.
[18] S. Winitzki, Uniform approximations for transcendental functions, in: International Conference on Computational Science and Its Applications, Springer, 2003, pp. 780–789.
[19] A. Jain, A. Kapoor, Exact analytical solutions of the parameters of real solar cells using Lambert W-function, Sol. Energy Mater. Sol. Cells 81 (2) (2004) 269–277.
[20] I. Nassar-Eddine, A. Obbadi, Y. Errami, M. Agunaou, et al., Parameter estimation of photovoltaic modules using iterative method and the Lambert W function: A comparative study, Energy Convers. Manage. 119 (2016) 37–48.
[21] E.I. Batzelis, G. Anagnostou, C. Chakraborty, B.C. Pal, Computation of the Lambert W function in photovoltaic modeling, in: ELECTRIMACS 2019, Springer, 2020, pp. 583–595.
[22] H.M. Ridha, Parameters extraction of single and double diodes photovoltaic models using Marine Predators Algorithm and Lambert W function, Sol. Energy 209 (2020) 674–693.
[23] M. Elyaqouti, E. Arjdal, A. Ibrahim, H. Abdul-Ghaffar, R. Aboelsaud, S. Obukhov, A.A.Z. Diab, et al., Parameters identification and optimization of photovoltaic panels under real conditions using Lambert W-function, Energy Rep. 7 (2021) 9035–9045.
[24] S. Pindado, E. Roibás-Millán, J. Cubas, J.M. Álvarez, D. Alfonso-Corcuera, J.L. Cubero-Estalrrich, A. Gonzalez-Estrada, M. Sanabria-Pinzón, R. Jado-Puente, Simplified Lambert W-function math equations when applied to photovoltaic systems modeling, IEEE Trans. Ind. Appl. 57 (2) (2021) 1779–1788.
[25] E. Moshksar, T. Ghanbari, A model-based algorithm for maximum power point tracking of PV systems using exact analytical solution of single-diode equivalent model, Sol. Energy 162 (2018) 117–131.
[26] E.I. Batzelis, I.A. Routsolias, S.A. Papathanassiou, An explicit PV string model based on the lambert W function and simplified MPP expressions for operation under partial shading, IEEE Trans. Sustain. Energy 5 (1) (2013) 301–312.
[27] S.-x. Lun, C.-j. Du, T.-t. Guo, S. Wang, J.-s. Sang, J.-p. Li, A new explicit I–V model of a solar cell based on Taylor's series expansion, Sol. Energy 94 (2013) 221–232.
[28] S.-x. Lun, C.-j. Du, G.-h. Yang, S. Wang, T.-t. Guo, J.-s. Sang, J.-p. Li, An explicit approximate I–V characteristic model of a solar cell based on padé approximants, Sol. Energy 92 (2013) 147–159.
[29] A.K. Das, An explicit J–V model of a solar cell using equivalent rational function form for simple estimation of maximum power point voltage, Sol. Energy 98 (2013) 400–403.
[30] S.-x. Lun, C.-j. Du, J.-s. Sang, T.-t. Guo, S. Wang, G.-h. Yang, An improved explicit I–V model of a solar cell based on symbolic function and manufacturer's datasheet, Sol. Energy 110 (2014) 603–614.
[31] S.-x. Lun, T.-t. Guo, C.-j. Du, A new explicit I–V model of a silicon solar cell based on Chebyshev Polynomials, Sol. Energy 119 (2015) 179–194.
[32] L.E. Mathew, A.K. Panchal, An exact and explicit PV panel curve computation assisted by two 2-port networks, Sol. Energy 240 (2022) 280–289.
[33] A. Bellini, S. Bifaretti, V. Iacovone, C. Cornaro, Simplified model of a photovoltaic module, in: 2009 Applied Electronics, IEEE, 2009, pp. 47–51.
[34] S. Jenkal, M. Kourchi, D. Yousfi, A. Benlarabi, M.L. Elhafyani, M. Ajaamoum, M. Oubella, Development of a photovoltaic characteristics generator based on mathematical models for four PV panel technologies, Int. J. Electr. Comput. Eng. (IJECE) 10 (6) (2020) 6101–6110.
[35] M.G. Villalva, J.R. Gazoli, E. Ruppert Filho, Comprehensive approach to modeling and simulation of photovoltaic arrays, IEEE Trans. Power Electron. 24 (5) (2009) 1198–1208.
[36] M.H. Mobarak, J. Bauman, A fast parabolic-assumption algorithm for global MPPT of photovoltaic systems under partial shading conditions, IEEE Trans. Ind. Electron. 69 (8) (2021) 8066–8079.
[37] A. Kouchaki, H. Iman-Eini, B. Asaei, A new maximum power point tracking strategy for PV arrays under uniform and non-uniform insolation conditions, Sol. Energy 91 (2013) 221–232.
[38] J. Ahmed, Z. Salam, An enhanced adaptive P&O MPPT for fast and efficient tracking under varying environmental conditions, IEEE Trans. Sustain. Energy 9 (3) (2018) 1487–1496.
[39] J.-Y. Park, S.-J. Choi, A novel simulation model for PV panels based on datasheet parameter tuning, Sol. Energy 145 (2017) 90–98.
[40] M. Bashahu, P. Nkundabakura, Review and tests of methods for the determination of the solar cell junction ideality factors, Sol. Energy 81 (7) (2007) 856–863.
[41] E. Meyer, Extraction of saturation current and ideality factor from measuring Voc and Isc of photovoltaic modules, Int. J. Photoenergy 2017 (2017).
[42] H. Bayhan, M. Bayhan, A simple approach to determine the solar cell diode ideality factor under illumination, Sol. Energy 85 (5) (2011) 769–775.
[43] F.A. Lindholm, J.G. Fossum, E.L. Burgess, Application of the superposition principle to solar-cell analysis, IEEE Trans. Electron Devices 26 (3) (1979) 165–171.
[44] J. Appelbaum, A. Peled, Parameters extraction of solar cells–A comparative examination of three methods, Sol. Energy Mater. Sol. Cells 122 (2014) 164–173.
[45] A. Ben Or, J. Appelbaum, Estimation of multi-junction solar cell parameters, Prog. Photovolt., Res. Appl. 21 (4) (2013) 713–723.
[46] D. Chan, J. Phillips, J. Phang, A comparative study of extraction methods for solar cell model parameters, Solid-State Electron. 29 (3) (1986) 329–337.
[47] D.S. Chan, J.C. Phang, Analytical methods for the extraction of solar-cell single- and double-diode model parameters from IV characteristics, IEEE Trans. Electron Devices 34 (2) (1987) 286–293.
[48] C. Chen, N. Strader, A normalized multidimensional Newton-Raphson method, Internat. J. Control 12 (2) (1970) 273–279.
[49] W.Y. Yang, W. Cao, J. Kim, K.W. Park, H.-H. Park, J. Joung, J.-S. Ro, H.L. Lee, C.-H. Hong, T. Im, Applied Numerical Methods Using MATLAB, John Wiley & Sons, 2020.
[50] J. Gow, C. Manning, Development of a photovoltaic array model for use in power-electronics simulation studies, IEE Proc.-Electr. Power Appl. 146 (2) (1999) 193–200.
[51] X.H. Nguyen, M.P. Nguyen, Mathematical modeling of photovoltaic cell/module/arrays with tags in Matlab/Simulink, Environ. Syst. Res. 4 (1) (2015) 1–13.
[52] E.I. Batzelis, S.A. Papathanassiou, A method for the analytical extraction of the single-diode PV model parameters, IEEE Trans. Sustain. Energy 7 (2) (2015) 504–512.
[53] H.K. Mehta, A.K. Panchal, PV panel performance evaluation via accurate V–I polynomial with efficient computation, IEEE J. Photovolt. 11 (6) (2021) 1519–1527.